

Non-isothermal Crystallization Behaviors of Coal Gangue/PBAT Composites Prepared via Solution Blending

Xiaoyang Liu¹, Dongyan Fan¹, Xu Li¹, Tao Du¹, Kezhen Qi², Dayi Qian¹ and Jianbin Song^{1,*}

¹Xinjiang Key Laboratory of Clean Conversion and High Value Utilization of Biomass Resources, School of Chemistry and Chemical Engineering, Yili Normal University, Yili 835000, China

²College of Pharmacy, Dali University, Dali 671000, Yunnan, China

Abstract: In order to lessen the environmental pollution caused by coal gangue and facilitate its utilization in the polymer industry, a study on the melting and crystallization behaviors of coal gangue/Polybutylene adipate terephthalate (PBAT) composites was conducted using a differential scanning calorimetry (DSC). The results indicate that a small amount of coal gangue enhances nucleation ability, perfection degree of PBAT crystals, and accelerates PBAT crystallization rate. However, excessive coal gangue hinders PBAT crystallization. These outcomes are confirmed by Crystallization Rate Coefficient (CRC) and Mandelkern method.

Keywords: Coal gangue, PBAT, Crystallization, DSC.

1. INTRODUCTION

Coal gangue, a byproduct generated during coal mining, is one of China's primary industrial solid wastes. The nation's accumulated coal gangue currently exceeds 8 billion tons and increases by 500 million tons annually [1]. This situation has significantly heightened the urgency for effective resource utilization and ecological management within the coal industry. Currently, coal gangue is mainly used in various fields, including cement production, road construction materials, mine filling materials [2], geopolymers [3], metal refining [4], fertilizers [5], adsorbent materials [6], polymer composites [7, 8], microwave absorbing materials [9], etc.

Coal gangue primarily consists of SiO_2 , Al_2O_3 , CaO , MgO , Fe_2O_3 , TiO_2 , and carbon. This unique chemical composition endows it with significant potential as a functional filler in polymer composites. However, research on coal-gangue-reinforced polymer materials remains scarce. The existing literature, though sparse, offers valuable insights into both the processing methodologies and practical applications of these sustainable composite systems. For example, Zhang *et al.* [10] observed that polyurethane (PU) improved the compressive strength of coal gangue. Li *et al.* [11] studied the effects of KH-550-treated coal gangue on the crystallization, melting and morphology of PE, and obtained some meaningful outcomes. Their work not only boosts the utilization of coal gangue waste but also paves the way for using coal gangue-polyethylene composite materials in the automotive industry. Liu *et al.* [12] prepared the of coal gangue/ethylene propylene

diene monomer (EPDM) /polypropylene (PP) ternary composites via a melting mixing method and found that incorporating coal gangue powder reduced the tensile strength and fracture toughness. Li *et al.* [13] synthesized polyacrylamide/hollow coal gangue spheres superabsorbent composites using solution polymerization, which displayed excellent water and salt absorption. In our prior study, we fabricated epoxy/coal gangue composites and found that optimal mechanical properties were achieved when the coal-gangue content reaches 80%.

PBAT is a biodegradable plastic featuring excellent flexibility, impact resistance, and dimensional stability. Owing to these properties, it has been extensively used in a variety of fields, including packaging, agricultural films, construction field, disposable tableware, and medical supplies [14-16]. PBAT can be combined with natural fibers, inorganic fillers, and other materials to create decorative panels for interior walls, ceilings, and other areas of buildings. This decorative panel not only has a beautiful appearance and good physical properties, but also reduces its impact on the environment. For example, PBAT foam material has the characteristics of low density, high porosity, good flexibility, efficient energy absorption, thermal insulation, excellent resilience, and environmental friendliness. In order to further improve the mechanical properties of PBAT foam materials, researchers usually incorporate some organic/inorganic fillers into PBAT matrix. He *et al.* [17] fabricated expandable graphite-modified straw fiber@PBAT foamed materials using a supercritical carbon dioxide technology. This composite material exhibits significant improvements in hardness, resilience, and compressive strength, along with inherent flame-retardant properties.

So, in this study, an eco-friendly approach to reduce environmental pollution from coal gangue is proposed.

*Address correspondence to this author at the Xinjiang Key Laboratory of Clean Conversion and High Value Utilization of Biomass Resources, School of Chemistry and Chemical Engineering, Yili Normal University, Yili 835000, China; E-mail: jianbin1102@163.com

Utilizing solution blending method, we systematically incorporated coal gangue into the biodegradable PBAT matrix. Differential scanning calorimetry (DSC) is employed to comprehensively analyze the influence of coal gangue on the melting behavior and crystallization kinetics of PBAT.

2. EXPERIMENTAL

2.1. Materials and Preparation

Polyethylene terephthalate adipic acid butyl ester (PBAT, TH801) was purchased from Xinjiang Lanshan Tunhe Co., Ltd (China). Coal gangue (200 μ m) was provided by Yili Xintian Coal Chemical Co., Ltd (China).

Firstly, to remove the carbon from the coal gangue, it was heated to 1000°C at a rate of 20°C /min in a muffle furnace. It was maintained at this temperature for 30 minutes before being naturally cooled to room temperature.

PBAT and coal gangue were mixed via solution blending. PBAT was first dissolved in N, N-dimethylformamide at 70°C to achieve a 15 wt % concentration. Coal gangue powder was then added to the PBAT solution and stirred for 15 min. The resulting mixture was dried in a vacuum oven at 60°C for 24 h to remove the solvent. The coal gangue content in the PBAT composites was set at 4 wt % and 8 wt %, labeled PBAT4 and PBAT8, respectively. To study coal gangue's effect on PBAT's melting and crystallization without interference from other additives, no additional agents were used in this study.

2.2. Characterization

The melting and crystallization of PBAT and its composites were analyzed using a DSC250 apparatus (TA Instruments, USA). Samples were heated from room temperature to 150°C at 10°C /min under nitrogen. They were held at 150°C for 5 minutes to erase thermal history, then cooled back to room temperature at controlled rates of 5°C /min, 10°C /min, 20°C /min, and 40°C /min. The entire process was recorded.

3. RESULTS

3.1. Melting and Crystallization Behaviors

Figure 1 illustrates DSC curves of PBAT and its composites during the heating process. Neat PBAT displays three melting peaks and one crystallization peak from low temperature to high temperature, locating at 44°C, 105°C, and 114°C, and a cold crystallization peak at 100°C. The low melting peak at 44°C is ascribed to unstable crystals formed during the evaporation of N, N - dimethylformamide at 70°C. The

peaks at 105°C and 114°C correspond to crystals melting and re-crystallization, respectively. The cold crystallization peak results from recrystallizing of uncrosslinked molecular chains upon heating. These complex melting behaviors indicate that PBAT formed crystals with different perfection levels during solution crystallization.

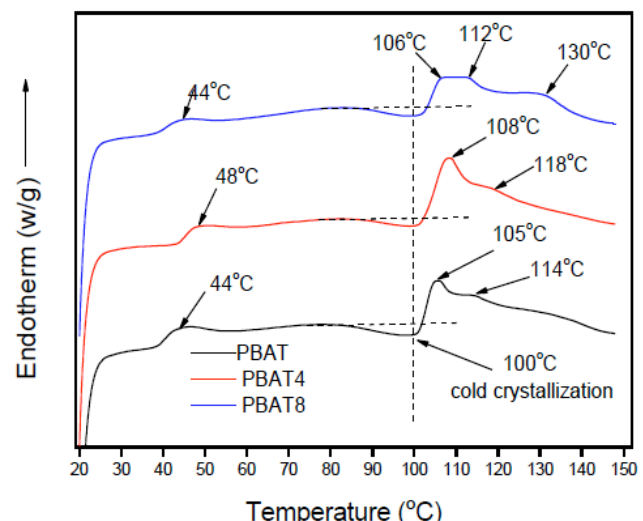


Figure 1: DSC curves of PBAT and its composites with a heating rate of 10°C/min.

As 4% of coal gangue is incorporated, the low melting peak, locating at 44°C for PBAT, shifts to 48°C. Meanwhile, the two melting peaks of PBAT4 move to 108°C and 118°C. Additionally, the melting peak area of PBAT4 increased compared to that of neat PBAT. These results suggest that the addition of coal gangue not only improved the perfection degree of PBAT crystals but also accelerated PBAT crystallization. However, when the content of coal gangue reaches 8wt%, the low melting peak drops back to 44°C again. At the same time, there is a plateau-shaped melting peak from 106°C to 112°C and one melting peak at 130°C on the DSC curve of PBAT8. Additionally, the melting peaks area of PBAT8 is smaller than that of PBAT and PBAT 4. This denotes excess coal gangue prohibits PBAT crystallization. It should be noted that, regardless of the coal gangue content, the cold crystallization peak at 100°C remains unchanged.

The impact of coal gangue on PBAT crystallization can be attributed to the following factors. Coal gangue is composed of multiple oxides, such as SiO_2 , Al_2O_3 , Fe_2O_3 , etc. These metal oxides strongly interact with the polar groups in PBAT, and this interaction causes PBAT molecular chains to be absorbed onto the surface of coal gangue and arranged regularly into crystals. Also, coal gangue can serve as a nucleation site for PBAT crystallization. Consequently, PBAT4 composites showed a higher melting point than that of neat PBAT (Figure 1). However, as coal gangue

content increase 8 wt%, PBAT8 exhibits complicated melting behaviors. The reason for this is due to the addition of excess coal gangue produce enhancing interactions between coal gangue and PBAT. Such strong interaction inhibits PBAT molecular chains from moving and aligning into crystals. Consequently, PBAT form some crystals with varying perfection degrees, leading to complicated melting behaviors on heating.

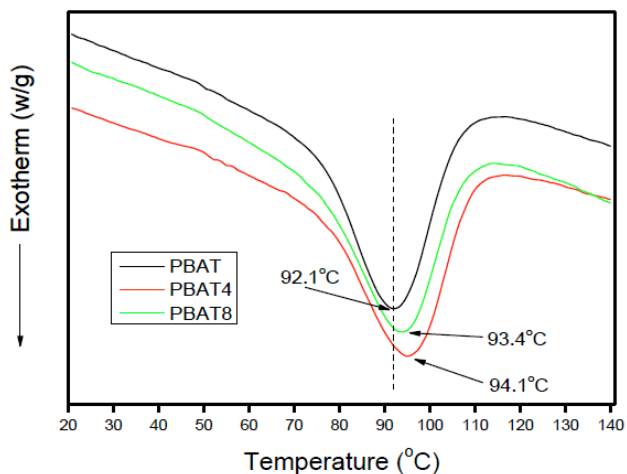


Figure 2: DSC curves of PBAT and its composites on cooling.

Figure 2 shows DSC cooling process of PBAT and its composites from 150°C to room temperature at a cooling rate of 5°C /min. It is widely acknowledged that the crystallization temperature of polymer is closely linked to its nucleation ability. The higher crystallization temperature suggests a stronger nucleation ability. As depicted in Figure 2, neat PBAT exhibits a crystallization temperature of 92.1°C, whereas PBAT composites containing 4 wt% and 8 wt% coal gangue show crystallization temperatures of 94.1°C and 93.4°C, respectively. This implies that coal gangue can enhance the nucleation ability of PBAT. However, it should be noted that an excessive amount of coal gangue may lead to a certain degree of decline in the nucleation ability.

3.3. Non-isothermal Crystallization Kinetics

In most cases, because polymer processing is carried out under non-isothermal conditions, temperature controlling plays an important role in the performance of polymer products. Figure 3 shows the cooling curves of PBAT and its composites with varying cooling rate. The data of crystallization temperature (T_c) and half-time for crystallization ($t_{1/2}$) are listed in Table 1. The T_c of the sample decreases as the cooling rate increases, which is due to polymer chain segments could not be timely response to the temperature variation, leading to a lag in the crystallization process. Interestingly, as coal gangue is added, the T_c first increases and then decreases at the same cooling rate.

The increase in T_c indicates enhanced nucleation ability.

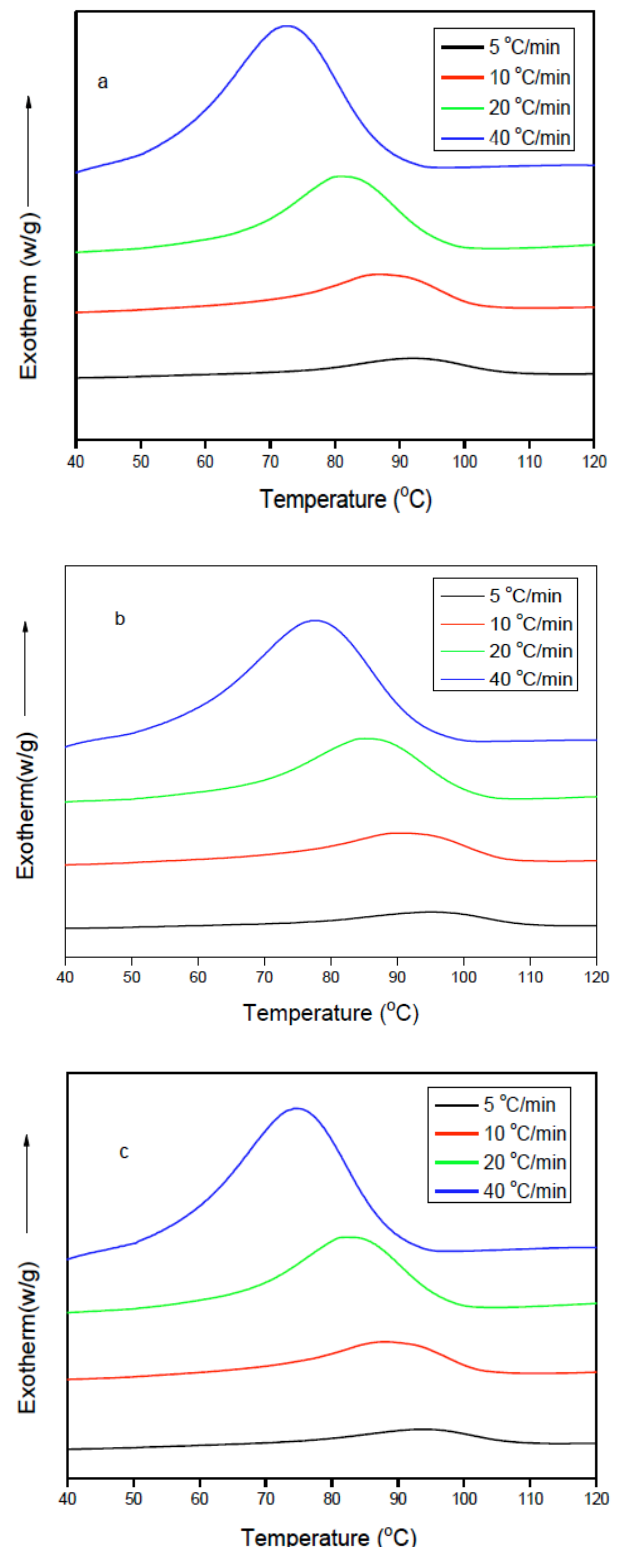


Figure 3: cooling curves of PBAT and its composites under various cooling rates. **a)** neat PBAT; **b)** PBAT4; **c)** PBAT8.

The half-time for crystallization ($t_{1/2}$) is an indicator of the overall crystallization rate, with a higher $t_{1/2}$ corresponding to a slower crystallization process. As shown in Table 1, the $t_{1/2}$ of the PBAT composites is lower than that of neat PBAT, indicating that the

addition of coal gangue accelerates the overall crystallization rate. This improvement is mainly attributed to the enhanced nucleation provided by the incorporated coal gangue. The coal gangue provides nucleation sites for PBAT crystallization and, through strong interactions with PBAT molecules, promotes their crystallization. However, an excess of coal gangue can hinder PBAT chains from moving and crystallizing, as evidenced by the higher $t_{1/2}$ of PBAT8 compared with PBAT4.

Table 1: Data of Crystallization Temperature (T_c) and $t_{1/2}$ of PBAT and its Composites

Samples	ϕ (°C/min)	T_c (°C)	$t_{1/2}$ (min)
Neat PBAT	5	92.1	6.38
	10	86.9	3.22
	20	80.7	1.38
	40	72.5	0.7
PBAT4	5	94.9	4.85
	10	90.6	2.70
	20	85.1	1.24
	40	77.9	0.50
PBAT8	5	93.4	5.95
	10	87.9	2.73
	20	82.1	1.32
	40	74.8	0.56

Crystallization Rate Coefficient (CRC)

In order to evaluate the crystallization ability, Khanna proposed a new parameter to study non-isothermal crystallization of polymer: crystallization rate coefficient, CRC [18]. This parameter has been successfully applied to many polymer systems [19-23].

$$\phi = CRC \times (T_m - T_c) = CRC \times \Delta T \quad (1)$$

Where ϕ is the cooling rate(°C·h⁻¹), T_m is the melting temperature(°C) and T_c is the crystallization temperature of samples(°C). By plotting ϕ versus ΔT , the CRC can be obtained from the slope, as shown in Figure 4. The larger the CRC value, the quicker the crystallization rate of polymer. The CRC values were calculated as 126.9 h⁻¹, 139.7 h⁻¹, 122.8 h⁻¹ for neat PBAT, PBAT4 and PBAT8, respectively. Evidently, the incorporation of coal gangue exerts a significant influence on the crystallization behavior of PBAT: a small amount of coal gangue accelerates PBAT crystallization, whereas an excessive amount hinders this process. These observations are consistent with the results of half-crystallization time ($t_{1/2}$) studies.

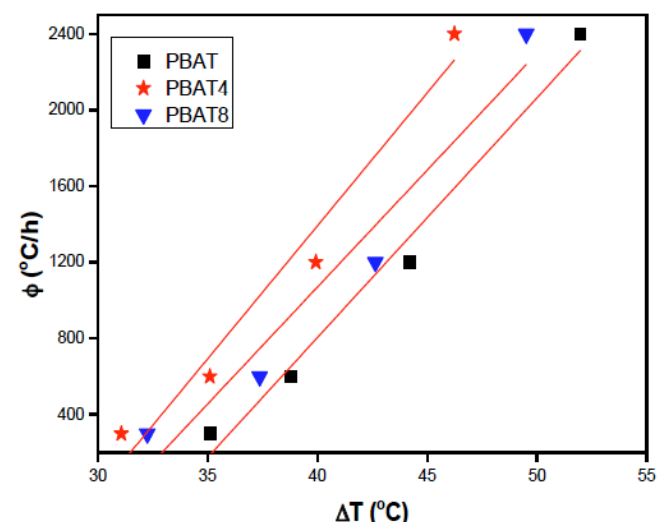


Figure 4: CRC of PBAT and its composite.

Mandelkern Method

For semi-crystalline polymers, temperature variations during processing exert a pronounced influence on crystallization behavior, which in turn governs the ultimate performance of the final products. In order to study such crystallization behaviors, Mandelkern proposed a method, assuming the crystallization temperature to be constant [24-26]. This method has been successfully applied to many polymers, such as polypropylene [27], polybutylene adipate terephthalate/polylactic acid blend [28], polytetrafluoroethylene [29], etc. In this study, the Avrami equation can be employed to investigate the primary stage of non-isothermal crystallization.

$$X(t) = 1 - \exp(-Z_t t^n) \quad (2)$$

This formula can be further written as:

$$\lg\{-\ln[1 - X(t)]\} = nlgt + \lg Z_t \quad (3)$$

Where X_t is the degree of crystallinity at the time t , Z_t is the crystallization rate constant in the non-isothermal process, and n is the Avrami exponent.

Considering the effect of the cooling rate, Jeziorny assumed ϕ to be approximately constant [25]. The final crystallization rate parameter (Z_c) is be further revised to:

$$\lg Z_c = \frac{\lg Z_t}{\phi} \quad (4)$$

Figure 5 shows the plots of $\lg(-\ln(1-X(t)))$ versus $\lg t$ of PBAT and its composites at different cooling rate. From the straight line at the initial crystallization stage, it can be obtained the parameters of n , Z_t and Z_c , and these data is shown in Table 2.

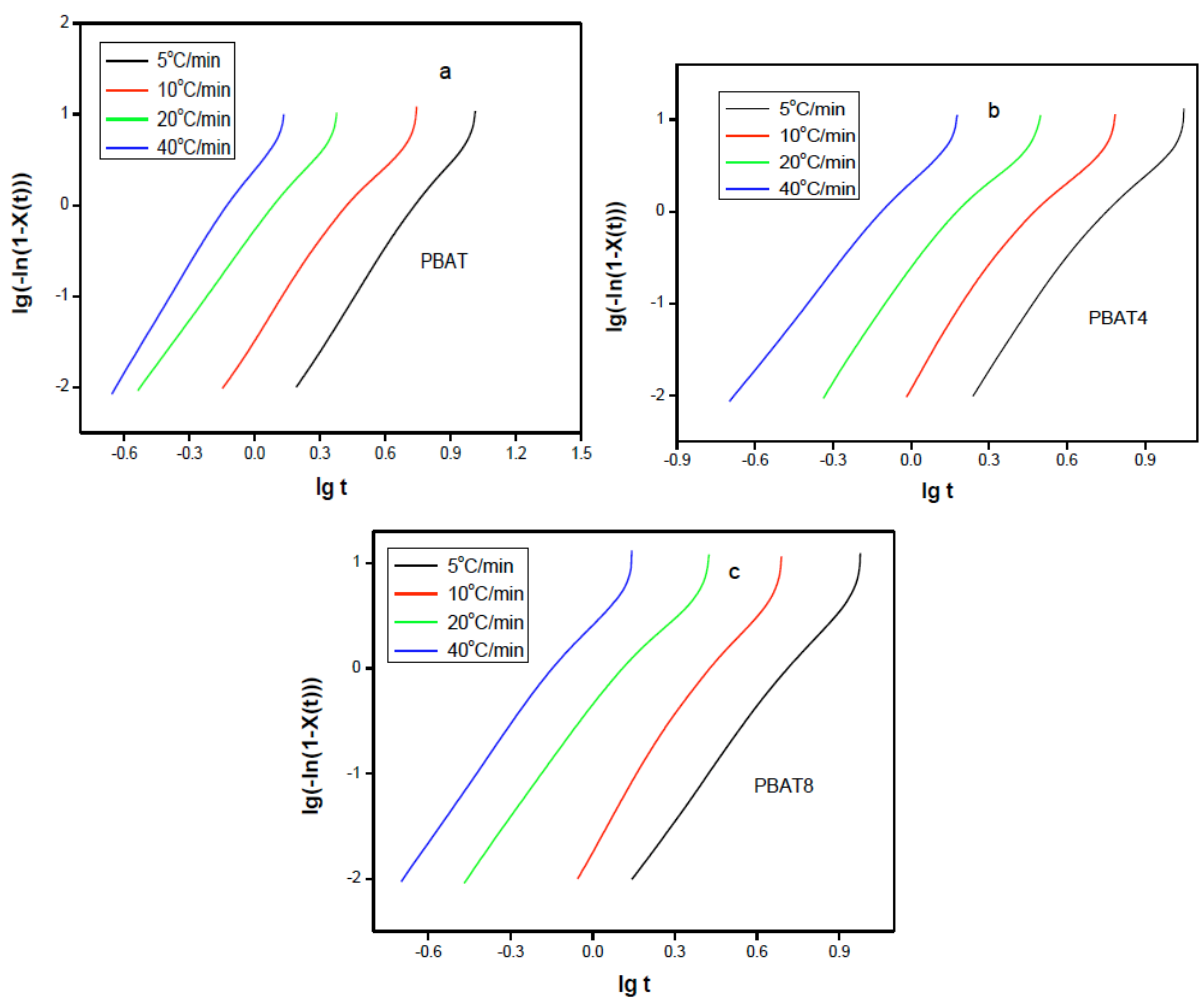


Figure 5: plots of $\lg(-\ln(1-X(t)))$ versus $\lg t$ of PBAT and its composites. **a)** neat PBAT; **b)** PBAT4; **c)** PBAT8.

From Table 2, The Avrami exponent n for PBAT and its composites is above 3, indicating that PBAT spherulites grow in a three-dimensional manner and the addition of coal gangue does not change growth mode of PBAT spherulites.

Table 2: The Data of n and Z_c Obtained by the Mandelkern Method

Samples	Cooling rate	n	Z_c
PBAT	5°C/min	3.7	0.28524
	10°C/min	3.6	0.71078
	20°C/min	3.2	0.90733
	40°C/min	3.9	1.00229
PBAT4	5°C/min	4.4	0.34563
	10°C/min	4.9	0.75161
	20°C/min	4.4	0.94048
	40°C/min	3.5	1.04026
PBAT8	5°C/min	3.5	0.31404
	10°C/min	4.7	0.73861
	20°C/min	3.7	0.92676
	40°C/min	3.7	1.03301

For every sample, the Z_c increases with increasing cooling rate, which is due to the increasing in supercooling. At the same cooling rate, PBAT4 has a higher value of Z_c than neat PBAT and PBAT8 do, indicating a quicker crystallization process at the initial stage. The reason is ascribed to the enhanced nucleation ability. It is noted that the Z_c of PBAT8 is lower than that of PBAT4. The reason is that excessive coal gangue inhibits PBAT chains from moving and aligning into crystals, which is uniformed with the CRC results.

Activation Energy of Non-isothermal Crystallization

Considering the changes in the crystallization temperature with the cooling rate, we can derive activation energy ΔE for non-isothermal crystallization by the Kissinger method [30-32]:

$$\frac{d \ln(\frac{\phi}{T^2})}{d(\frac{1}{T})} = -\frac{\Delta E}{R} \quad (5)$$

where T is the crystallization temperature of samples, shown in Table 1. From Figure 6, the activation energy of PBAT, PBAT4 and PBAT8 are determined to be

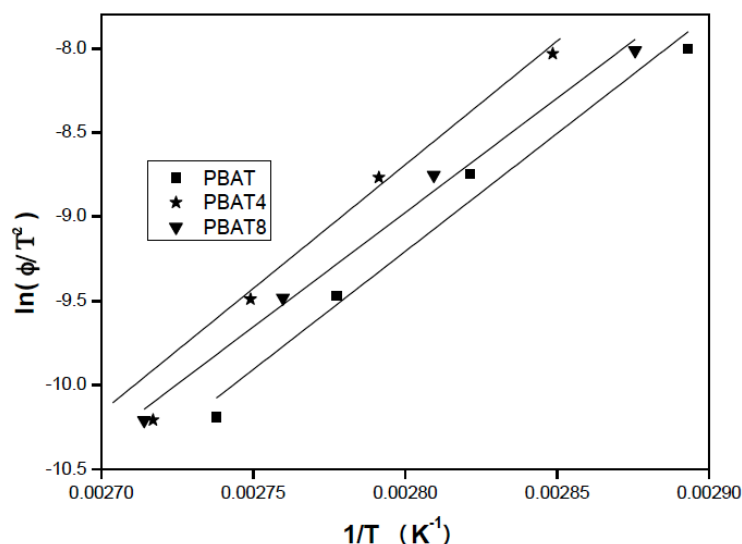


Figure 6: Plot of $\ln(\phi/T^2)$ versus $1/T$ from the Kissinger method.

131.3 KJ/mol, 132.1 KJ/mol and 130.9 KJ/mol, respectively. It can be seen that the addition of coal gangue did not affect the activation energy of PBAT, and these results have proved the Kissinger method was not suitable for handling such complex systems.

4. CONCLUSION

In this study, differential scanning calorimetry (DSC) was employed to investigate the non-isothermal crystallization kinetics of coal gangue/PBAT composites, which were fabricated via solution blending. The findings reveal that a small amount of coal gangue improves the perfection degree of crystals and nucleation ability of PBAT. The PBAT's melting temperature increases from 105°C to 108°C and its crystallization temperature is elevated from 92.1°C to 94.9°C. Furthermore, the CRC of PBAT and its composites is determined to be 126.9/h, 139.7/h, 122.8/h for PBAT, PBAT4, and PBAT8 respectively. The analysis of non-isothermal crystallization kinetics indicates PBAT crystals grow in a three-dimensional manner and coal gangue increases PBAT crystallization rate. the non-isothermal crystallization energy of PBAT changes only slightly regardless of the coal gangue content, which means that the Kissinger method is not applied to coal gangue/PBAT system.

ACKNOWLEDGMENT

This research was supported by the Special Project for Enhancing the Comprehensive Strength of Disciplines at Yili Normal University (22XKZZ15); Key R & D Project of Xinjiang Science and Technology Department (2023B01014).

CONFLICTS OF INTEREST

The authors declare that they have no known competing financial interests or personal relationships

that could have appeared to influence the work reported in this paper.

REFERENCES

- [1] Zhao Y, Yang C, Li K, et al. Toward understanding the activation and hydration mechanisms of composite activated coal gangue geopolymers [J]. *Construction and Building Materials*, 2022, 318: 1567. <https://doi.org/10.1016/j.conbuildmat.2021.125999>
- [2] Qin Z, Jin J, Lü X. Insights into mechanical property and damage evaluation of a novel waste-based coal gangue-filled backfill [J]. *Construction and Building Materials*, 2023, 389: 131802. <https://doi.org/10.1016/j.conbuildmat.2023.131802>
- [3] Feng D, Wang J, Wang Y. Alkali-activated geopolymers prepared from coal gangue and municipal solid waste incineration byproducts [J]. *Journal of Building Engineering*, 2023, 80(1): 108074. <https://doi.org/10.1016/j.jobe.2023.108074>
- [4] Qin Q, Geng H, Deng J. Al and other critical metals co-extraction from coal gangue through delamination pretreatment and recycling strategies [J]. *Chemical Engineering Journal*, 2023, 477: 147036. <https://doi.org/10.1016/j.cej.2023.147036>
- [5] Zhu X, Gong W, Wang L. Reclamation of waste coal gangue activated by *Stenotrophomonas maltophilia* for mine soil improvement: Solubilizing behavior of bacteria on nutrient elements [J]. *Journal of Environmental Management*, 2022, 320: 115865. <https://doi.org/10.1016/j.jenvman.2022.115865>
- [6] Mei Y, Pang J, Wang X, et al. Coal gangue geopolymers as sustainable and cost-effective adsorbents for efficient removal of Cu (II) [J]. *Environmental Technology & Innovation*, 2023, 32: 103416. <https://doi.org/10.1016/j.eti.2023.103416>
- [7] Gong G, Xie B, Yang M, et al. Mechanical properties and fracture behavior of injection and compression molded polypropylene/coal gangue powder composites with and without a polymeric coupling agent [J]. *Composites: Part A*, 2007, 38: 1683-1693. <https://doi.org/10.1016/j.compositesa.2007.02.002>
- [8] Li C, Liao H, Gao H, et al. A facile green and cost-effective manufacturing process from coal gangue-reinforced composites [J]. *Composites Science and Technology*, 2023, 233: 109908. <https://doi.org/10.1016/j.compscitech.2023.109908>
- [9] Wang Y, Liang L, Zhu B, et al. Economical preparation of $\text{Fe}_3\text{O}_4/\text{C}/\text{CG}$ and $\text{Fe}/\text{C}/\text{CG}$ composites as microwave

absorbents by recycling of coal gangue [J]. Materials Research Bulletin, 2022, 146: 111573.
<https://doi.org/10.1016/j.materresbull.2021.111573>

[10] Zhang W, Yang H, Zhang S, et al., Study on comprehensive properties of polyurethane used as curing material of coal gangue, Science of Soil and Water Conservation, 2024, 22(3):109-119.

[11] Li C, Liao H, Gao H, et al., Enhancing interface compatibility in high-filled coal gangue/polyethylene composites through silane coupling agent-mediated interface modification, Composites Science and Technology, 2024, 251:110546.
<https://doi.org/10.1016/j.compscitech.2024.110546>

[12] Liu Y, Xie B, Yang W, et al. The composition, morphology, and mechanical properties of ethylene propylene diene monomer-encapsulated coal gangue powder/polypropylene composites. Polymer Composites, 2010, 31(1): 10-17.
<https://doi.org/10.1002/pc.20804>

[13] Li Y, Ren N, Wang Y, et al., Synthesis and properties of polyacrylamide/hollow coal gangue spheres superabsorbent composites. Journal of Applied Polymer Science, 2013, 130(3): 2184-2187.
<https://doi.org/10.1002/app.39441>

[14] Miguel G, Aimee A H, Adriana B E. Modeling and optimization of mechanical, water vapor permeability and haze properties of PLA and PBAT films reinforced with montmorillonite, halloysite nanotubes and palygorskite using artificial neural networks and genetic algorithms. Food Packaging and Shelf Life, 2025, 49:101533.
<https://doi.org/10.1016/j.fpsl.2025.101533>

[15] Sivanantham G, Divakaran D, Suyambulingam I, et al., Isolation and characterization of microcrystalline cellulose from rice stalk agro-waste and its application in enhancing inherent properties of PBAT biofilm. Process Safety and Environmental Protection, 2025, 196: 106864.
<https://doi.org/10.1016/j.psep.2025.106864>

[16] Liu J, Zhang X, Wang H, et al., Study on the Improvement of Foaming Properties of PBAT/PLA Composites by the Collaboration of Nano- Fe_3O_4 Carbon Nanotubes. Journal of Renewable Materials, 2025, 13(4), 669-685.
<https://doi.org/10.32604/jrm.2025.02025-0042>

[17] He Y, Shao L, Liu M, et al. Preparation and properties of expandable graphite-modified straw fiber[®]PBAT foamed bead composites. Fine Chemicals, 2025, 42(1): 103-110.

[18] Khanna, Y. P. A barometer of crystallization rates of polymeric materials. Polym. Eng. Sci., 1990, 30(24), 1615-1619.
<https://doi.org/10.1002/pen.760302410>

[19] Song J, Chen Q, Ren M, et al., Effect of Partial Melting on the Crystallization Kinetics of Nylon-1212. Journal of Polymer Science: Part B: Polymer Physics, 2005, 43: 3222-3230.
<https://doi.org/10.1002/polb.20525>

[20] Li J, Qiu Z. Nonisothermal Melt Crystallization Study of Poly(ethylene succinate)/Cellulose Nanocrystals Composites. Journal of Polymers and the Environment, 2022, 30:1518-1527.
<https://doi.org/10.1007/s10924-021-02294-0>

[21] Chen T, Zhang J. Non-isothermal cold crystallization kinetics of poly(ethylene glycol-co-1,4-cyclohexanedimethanol terephthalate) (PETG) copolymers with different compositions. Polymer Testing, 2015, 48: 23-30.
<https://doi.org/10.1016/j.polymertesting.2015.09.008>

[22] Tjong S. C, Xu S. Ai. Non-isothermal crystallization kinetics of calcium carbonate-filled β -crystalline phase polypropylene composites. Polymer International, 1997, 44(1): 95-103.
[https://doi.org/10.1002/\(SICI\)1097-0126\(199709\)44:1<95::AI>2.3.CO;2-L](https://doi.org/10.1002/(SICI)1097-0126(199709)44:1<95::AI>2.3.CO;2-L)

[23] Razavi-Nouri M, Salavati M. Physico-mechanical properties of poly(ethylene-co-vinyl acetate)/acrylonitrile-butadiene rubber/multi-walled carbon nanotubes nanocomposites. Polymer composites, 2025, 43(7): 4358-4370.
<https://doi.org/10.1002/pc.26697>

[24] Fava, R. A. Methods of Experimental Physics; Academic: New York, 1980, p 16.

[25] Zhang, Q. X.; Zhang, Z. H.; Zhang, H. F.; Mo, Z. S. J Polym Sci Part B: Polym Phys 2002, 40, 1790-1791.
<https://doi.org/10.1002/polb.10114.abs>

[26] Zhang S, Wang Z, Guo B, et al., Secondary nucleation in polymer crystallization: A kinetic view. Polymer Crystallization, 2021, 4(3): doi.org/10.1002/pcr2.10173.
<https://doi.org/10.1002/pcr2.10173>

[27] Macedo T C P, Campos D A T, Lima T N, et al., Non-isothermal Crystallization Kinetics, Thermal, and Rheological Behavior of Linear/Branched Polypropylene Blends. Macromolecular Symposia, 2022, 406(1).
<https://doi.org/10.1002/masy.202200042>

[28] Zhao Z, Balu R, Choudhury N R, et al., The effect of tetra-needle-like zinc oxide whisker as additive on the crystallization kinetics of polybutylene adipate terephthalate/polylactic acid blend. Polymer Engineering & Science, 2024, 64(9): 4079-4098.
<https://doi.org/10.1002/pen.26834>

[29] Wang X, Huang G, Zhou S, et al., Effect of crystallization behavior on wear properties of polytetrafluoroethylene composites modified by irradiation above melting point. Polymer composites, 2025, 46(1): 809-816.
<https://doi.org/10.1002/pc.29026>

[30] Kissinger, H. E. Variation of peak temperature with heating rate in differential thermal analysis. J. Res. Natl. Bur. Stand., 1956, 57, 217-222.
<https://doi.org/10.6028/jres.057.026>

[31] Svboda R, Machotová J. How Depolymerization-Based Plasticization Affects the Process of Cold Crystallization in Poly(P-Dioxanone). Macromolecular Rapid Communications, 2024, 45(20).
<https://doi.org/10.1002/marc.202400369>

[32] Dantas L, Araújo A, Barros J, et al., Using Urban Residue in Polylactic Acid Composites Part I: Effect of Castor Oil on the Crystallization Kinetics, Macromolecular Reaction Engineering, 2024, 19(2).
<https://doi.org/10.1002/mren.202400039>

<https://doi.org/10.66000/2819-828X.2025.01.03>

© 2025 Liu et al.

This is an open-access article licensed under the terms of the Creative Commons Attribution License (<http://creativecommons.org/licenses/by/4.0/>), which permits unrestricted use, distribution, and reproduction in any medium, provided the work is properly cited.